(This is a sample cover image for this issue. The actual cover is not yet available at this time.)

Intermetallics 22 (2012) 106–109

Contents lists available at SciVerse ScienceDirect

Intermetallics

journal homepage: www.elsevier.com/locate/intermet

Short communication

Crystal structure and magnetic properties of $GdZn_2Ga_2$

Yu. Verbovytskyy [a,*], K. Łątka [b], J. Przewoźnik [c], A.P. Gonçalves [a]

[a] Instituto Tecnológico e Nuclear/CFMC-UL, Estrada Nacional 10, P-2686-953 Sacavém Codex, Portugal
[b] M. Smoluchowski Institute of Physics, Jagiellonian University, Reymonta 4, 30-059 Kraków, Poland
[c] Department of Solid State Physics, Faculty of Physics and Applied Computer Science, AGH University of Science and Technology, Av. Mickiewicza 30, 30-059 Kraków, Poland

ARTICLE INFO

Article history:
Received 1 September 2011
Received in revised form
12 October 2011
Accepted 14 October 2011
Available online

Keywords:
A. Rare-earth intermetallics
B. Crystal chemistry of intermetallics
B. Phase identification
B. Magnetic properties
F. Diffraction

ABSTRACT

Gadolinium dizinc digallide, $GdZn_2Ga_2$, has been synthesized by reacting the elements at ~950 °C, followed by annealing at 400 °C. The crystal structure was solved from single crystal X-ray diffraction data ($a = 4.1305(4)$, $c = 10.775(2)$ Å, $V = 183.83(4)$ Å^3, $BaAl_4$ structure type, $I4/mmm$ space group, Pearson symbol $tI10$, $Z = 2$). This ternary compound undergoes a transition from a paramagnetic to an antiferromagnetic state at $T_N = 17.0$ K.

1. Introduction

Ternary representatives with tetragonal $BaAl_4$ structure type form a large group among systems with rare earths (R), transition metals (T) and *p*-elements from IIIA–VA subgroups (X) [1]. Numerous examples of $BaAl_4$-type related structures exist, with a different arrangement of the atoms and mainly with RT_2X_2 or RTX_3 compositions: $BaGa_2P_2$, $BaMg_2Sn_2$, $BaNi_2Si_2$, $BaPt_2Ge_2$, $CaBe_2Ge_2$, $CeAl_2Ga_2$, $EuGa_2P_2$, $LaPt_2Ge_2$, $BaNiSn_3$, $CePtGa_3$, $CaCu_{0.15}Ga_{3.85}$, $CaGa_4$, $URh_{2-x}As_{2-y}$, $CeCu_{2-x}In_{2-y}$, $CeNi_{2.36}Sb_{1.64}$, $LaPt_{1.42}Pd_{0.58}Ge_2$, $SrMgIn_2$ $YAl_{2.6}Ga_{1.4}$ and $YAl_{1.8}Ga_{2.2}$ [2]. Depending on the nature of forming elements, the existence of deformed cases (superstructures) is also typical for such systems.

Recently, we present some results on the interaction among the components from ternary rare earth, zinc and gallium systems. Studies on Yb–Zn–Ga system, isothermal section at 400 °C and formation of new ternary compounds can be found in [3–5]. Crystal structure and magnetic properties of RZn_2Ga_2 (R = La, Ce, Pr, Nd, Sm and Eu) phases were already published in [6,7]. Phase identification and crystal structure of $RZn_{2-x}Ga_{2+x}$, $R_3Zn_{11-x}Ga_x$ and $RZn_{11-x}Ga_x$ with heavy rare earth metals (R = Y, Lu, Gd–Tm) were also given in [8]. Here, we present the crystal structure determination, based on single crystal X-ray diffraction data, and magnetic properties of the new $GdZn_2Ga_2$ intermetallic compound.

2. Experimental details

Starting materials for the $GdZn_2Ga_2$ alloy preparation were metals with nominal purities >99.95 wt.% (gadolinium ingots, zinc tear drops and gallium pieces). The reaction was performed at ~950 °C inside quartz ampoule under vacuum (10^{-5} Torr) for 1 h, followed cooling down in air. The obtained sample resulted as soft reaction product containing plated-like crystals with metallic luster. Finally, the ingot was cut into small pieces, sealed in an evacuated quartz tube and annealed at 400 °C for 30 days. After the heat treatment, the sample was quenched, by submerging the quartz tube into cold water.

Plated-like single crystals were extracted from the as-prepared and annealed $GdZn_2Ga_2$ alloys, and analyzed. Single crystal intensity data were collected at room temperature using a four-circle Enraf–Nonius Mach III diffractometer with graphite monochromatized Mo Kα-radiation and a scintillation counter with pulse height discrimination. Scans were taken in the $\omega/2\theta$ mode. Empirical absorption corrections were applied on the basis of Ψ-scan data. Crystal structure was successfully refined using Shelxl–97 [9] (full-matrix least-squares on F^2), confirming the tetragonal $BaAl_4$ structure type. The crystallographic data and experimental details are presented in Table 1. Final atom coordinates and displacement

* Corresponding author.
E-mail address: yuryvv@bigmir.net (Yu. Verbovytskyy).

0966-9795/$ – see front matter © 2011 Elsevier Ltd. All rights reserved.
doi:10.1016/j.intermet.2011.10.012

Table 1
Crystal data and structure refinement for $GdZn_2Ga_2$ (as-cast (**I**) and annealed (**II**)).

Empirical formula	$GdZn_2Ga_2$ (**I**)	$GdZn_2Ga_2$ (**II**)
Structure type	$BaAl_4$	$BaAl_4$
Crystal system	Tetragonal	Tetragonal
Space group	*I*4/*mmm*	*I*4/*mmm*
Pearson symbol	*tI*10	*tI*10
Cell parameters		
a	4.1320(4) Å	4.1305(4) Å
c	10.797(2) Å	10.775(2) Å
V	184.34(5) Å^3	183.83(4) Å^3
Formula units per cell	2	2
Calculated density	7.779 g/cm^3	7.801 g/cm^3
Crystal shape and colour	Plate, Silvery	Plate, Silvery
Diffractometer	Enraf–Nonius Mach III	Enraf–Nonius Mach III
Wavelength	Mo–K_α (λ = 0.71073 Å)	Mo–K_α (λ = 0.71073 Å)
Monochromator	Graphite	Graphite
Temperature	293(2) K	293(2) K
Absorption coefficient	45.525 mm^{-1}	45.652 mm^{-1}
F(000)	374	374
θ range for data collection	3.77°–44.94°	3.78°–44.97°
Scan type	ω–2θ	ω–2θ
Range in *hkl*	±8, ±8, ±21	±8, ±8, ±20
Total no. reflections	2824	2824
Independent reflection	251	260
Reflections with $I > 2\sigma(I)$	215	220
Structure refinement	SHELXL–97 (Sheldrick –1997)	SHELXL–97 (Sheldrick –1997)
Refinement method	Full–matrix least–squares on F^2	Full–matrix least–squares on F^2
Data/restraints/parameters	251/0/9	260/0/9
Goodness–of–fit on *F*	1.087	1.084
Final *R* indices[a]	$R1 = 0.0474$, $wR2 = 0.1125$	$R1 = 0.0489$, $wR2 = 0.0947$
R indices (all data)	$R1 = 0.0586$, $wR2 = 0.1201$	$R1 = 0.0616$, $wR2 = 0.0993$

[a] $R1 = \sum(||F_o| - |F_c||)/\sum|F_o|$, $wR2 = \{\sum w[(F_o^2 - F_c^2)^2]/\sum w[(F_o^2)^2]\}^{1/2}$; $w = 1/[\sigma^2(F_o^2)+(aP)^2 + bP]$, in which $P = (F_o^2 + 2F_c^2)/3]$.

parameters are given in Tables 2 and 3. Statistical mixtures of Zn and Ga were fixed during the refinement, as they are not distinguishable by X-ray diffraction.

Detailed bulk magnetisation measurements were made in the DC mode at the fields 50 Oe, 1 kOe as well as hysteresis loop up to 90 kOe were made in the temperature range 1.9 K up to 300 K using the vibrating sample magnetometer (VSM) option of the Quantum Design physical property measurement system (PPMS) and a roughly sphere-like sample. Especially, the measurements with VSM option at low external field $H_0 = 50$ Oe were applied since they enable investigations not significantly affecting the magnetic system, and therefore they are well suited for a precise determination of magnetic phase transitions. The right zeroing of the magnetic field was made using the ultra-low field VSM option. In the zero field cooling mode (ZFC) the sample was first cooled down in absence of external magnetic field and then investigated while heating in a given magnetic field. On the other hand, the field-cooling mode (FC) followed ZFC one in the same magnetic field and measurements were performed with decreasing temperature. For both modes, the cooling process always started from the paramagnetic state. The magnetic transition temperature was derived using numerical analysis of the obtained ZFC mass magnetisation curve σ(T). During magnetic measurements step scanning was applied both for temperature as well as for the field variations.

Table 2
Atom coordinates and isotropic displacement parameters for $GdZn_2Ga_2$ (**I** and **II**).

Atom	Site	*x*	*y*	*z*	U_{eq} (Å^2)
Gd	2a	0	0	0	0.0077(3)
		0	0	0	0.0090(2)
M1	4d	0	½	¼	0.0107(3)
		0	½	¼	0.0120(3)
M2	4e	0	0	0.38783(15)	0.0084(3)
		0	0	0.38761(15)	0.0100(3)

M1 = M2 = 0.5Zn + 0.5Ga. Data from first and second rows for as-cast and annealed $GdZn_2Ga_2$, respectively.

Table 3
Anisotropic displacement parameters for $GdZn_2Ga_2$ (**I** and **II**).

Atom	*U*11	*U*22	*U*33	*U*23	*U*13	*U*12
Gd	0.0070(3)	0.0070(3)	0.0093(4)	0	0	0
	0.0082(2)	0.0082(2)	0.0105(4)			
M1	0.0113(4)	0.0113(4)	0.0096(6)	0	0	0
	0.0126(4)	0.0126(4)	0.0108(6)			
M2	0.0098(4)	0.0098(4)	0.0054(6)	0	0	0
	0.0109(3)	0.0109(3)	0.0081(6)			

3. Results and discussion

3.1. Crystal structure

The new ternary gadolinium dizinc digallide, $GdZn_2Ga_2$, crystallizes with tetragonal $BaAl_4$ structure type (*I*4/*mmm* space group, Pearson symbol *tI*10, $Z = 2$). Gadolinium atoms occupy the position of Ba (2*a*) site, while the statistical mixture (M1 and M2) of the zinc and gallium atoms are at Al (the basal 4*d* and the apical 4*e*) sites. The M1 atoms at the basal site form two-dimensional square nets, which, together with the apical M2 atoms, form square pyramidal layers. The above mentioned layers are connected to each other along *c* axes, creating three-dimensional [ZnGa] network (Fig. 1). The neighbours of gadolinium atoms form 22-vertex polyhedra. The M1 atoms are located inside distorted cubooctahedra (coordination number 12). The coordination spheres of the M2 atoms have a form of one-capped tetragonal antiprisms (coordination number 9) [8]. Significantly shorter distances (less than sum of the atomic radii of respective atoms [10]) in the structure of $GdZn_2Ga_2$ have been found for Gd–M2 (3.162(1) Å), M1–M2 (2.542(1) Å) and M2–M2 (2.422(2) Å). They are close to the early published ones for $RZn_{2-x}Ga_{2+x}$ phases [6–8].

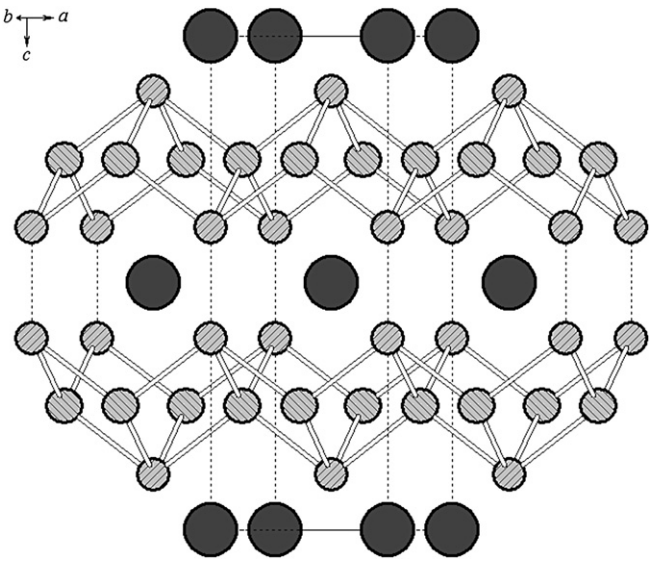

Fig. 1. Crystal structure of $GdZn_2Ga_2$. Dark circles indicate Gd atoms. Light (left and right) hatching circles are M1 and M2 (Zn and Ga) atoms, respectively.

3.2. Bulk magnetic properties

The temperature dependencies of the magnetic mass susceptibility $\chi_\sigma(T)$ and its inverse $1/\chi_\sigma(T)$ measured in a field of $H_0 = 1000$ Oe is presented in Fig. 2. The best fit to $\chi_\sigma(T)$ by a modified Curie–Weiss law in the form $\chi_\sigma = \chi_0 + C/(T - \theta_P)$, that can be obtained between 36 K and 300 K, gives the temperature independent factor $\chi_0 = 3.68 \cdot 10^{-6}$ cm^3/g, the Curie constant $C = 1.984 \cdot 10^{-2}$ K cm^3/g and the paramagnetic Curie temperature $\theta_P = -9.1$ K. The clearly negative value of Θ_p is indicative for antiferromagnetic interactions. The effective magnetic moment was derived from the formula $\mu_{eff} = p_{eff} \cdot \mu_B$, where $p_{eff} = (3k_B/N_A)^{1/2} \cdot (MC)^{1/2}/\mu_B$ (k_B is the Boltzmann constant, N_A is the Avogadro number and M is the molar mass expressed in grams). The experimental value $\mu_{eff} = 8.24\mu_B$ is slightly higher than the theoretical free-ion value $\mu_{eff} = g\mu_B[J(J+1)]^{1/2} = 7.94\mu_B$ for Gd^{3+} with $g = 2$ and $J = 7/2$. This was also observed for some isotypic GdT_2Si_2 intermetallics [11]. Such a behaviour might be explained in terms of strong coupling (polarization) of the conduction electrons with the gadolinium localized 4*f* moments. The excess moment, of the order of $0.3\mu_B$/Gd, observed here, could be mainly associated with the gadolinium *5d* delocalized electrons. It is induced, at least in part, due to *4f–5d* exchange interactions. In this case, the excess magnetic moment is correlated with 4*f* magnetic moment, therefore, $\mu_{eff} = \mu^{(4f)} + \mu^{(5d)}$ [11 and references therein]. Taking advantage of the values for $\mu_{eff} = 8.24\mu_B$/Gd and $\mu^{(4f)} = 7.94\mu_B$/Gd, one yields the results for $\mu^{(5d)} = (0.3 \pm 0.10)\ \mu_B$/Gd, a quite reasonable value. The *4f–5d*-exchange parameter is positive and the polarization of *5d*-band is enhanced by intraband interactions [12]. Thus, the susceptibility of *5d* electrons seems to play a dominant role in conduction electron polarization in the vicinity of the gadolinium ion.

The arrow in Fig. 2 points to the antiferromagnetic transition temperature $T_N = 17.0$ K, as obtained from the temperature dependence of the low field ZFC mass susceptibility recorded at $H_0 = 50$ Oe by means of a VSM option (see Fig. 3), which coincides fairly well with the antiferromagnetic maximum of the $\chi_\sigma(T)$ curve. Temperature variations of field-cooled (FC) and zero-field-cooled (ZFC) mass magnetisations measured at the low static field $H_0 = 50$ 0e are shown in Fig. 3 and both recorded curves fits altogether almost exactly. Numerical analysis of the first and the second derivatives obtained for the ZFC curve point to the

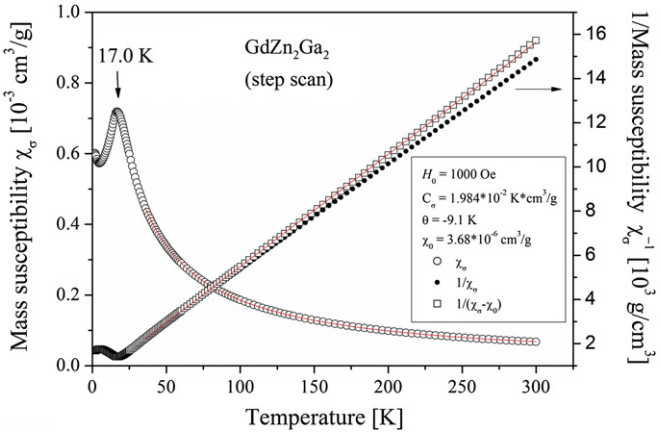

Fig. 2. Temperature dependence of the magnetic susceptibility (left-hand scale) and inverse susceptibility (right-hand scale) as measured with a PPMS using VSM for $GdZn_2Ga_2$ in an external magnetic field $H_0 = 1000$ Oe. In the inset, the magnetic parameters obtained from the fit represented by continuous line according to a modified Curie–Weiss law are presented, as explained in the text. The observed maximum at $T = 16.8$ K agrees well with $T_N = 17.0$ K as obtained from the low field magnetic measurements (see Fig. 3).

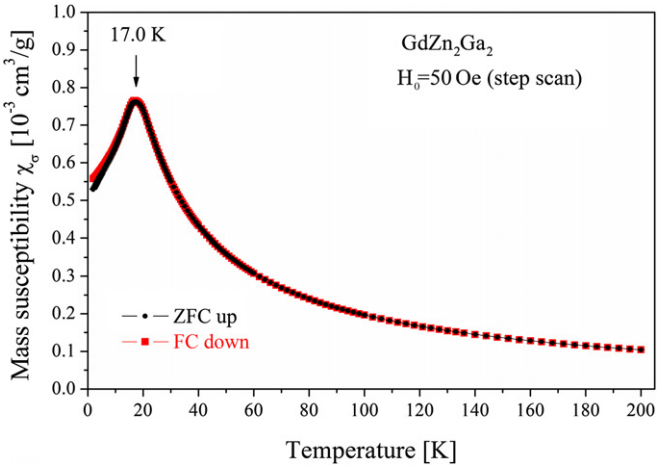

Fig. 3. Temperature dependence of the magnetic susceptibility as measured with a PPMS using low field VSM option for $GdZn_2Ga_2$ in an external magnetic field $H_0 = 50$ Oe. ZFC curve was recorded with rising temperature while FC one with decreasing temperature. Arrow point to the Néel temperature $T_N = 17.0$ K as explained in the text.

antiferromagnetic transition that takes place at the Néel temperature $T_N = 17.0$ K. Antiferromagnetic-type transitions were also observed before on other RZn_2Ga_2 (R = rare earth) zinc gallides crystallizing with the $BaAl_4$-type structure [6]: $PrZn_2Ga_2$ orders antiferromagnetically at $T_N = 7$ K, which is supported by a metamagnetic transition observed at low temperatures; $NdZn_2Ga_2$ orders antiferromagnetically, with $T_N = 3$ K, but below 2K an upturn in the magnetic susceptibility is observed, which may be due to spin reorientation; $SmZn_2Ga_2$ exhibits antiferromagnetism below $T_N = 16$ K, with also an upturn in the magnetic susceptibility below 5 K. On the other hand, the Eu divalent $EuZnGa_3$ and $EuZn_{1.25}Al_{2.75}$ phases (also with the $BaAl_4$-type structure) show a ferromagnetic-type behaviour, with Curie temperatures of 14(1) K and 25(2) K, respectively [7], and the $YbZn_xGa_{4-x}$ and $Yb_3Zn_{11-x}Ga_x$ phases present a diamagnetic behaviour [5].

Fig. 4 shows the magnetisation curve as a function of the magnetic field at temperature $T = 1.9$ K (i.e. much below the Néel temperature). It presents an almost reversible mass magnetisation $\sigma(H)$ dependence typical for antiferromagnetic-like materials.

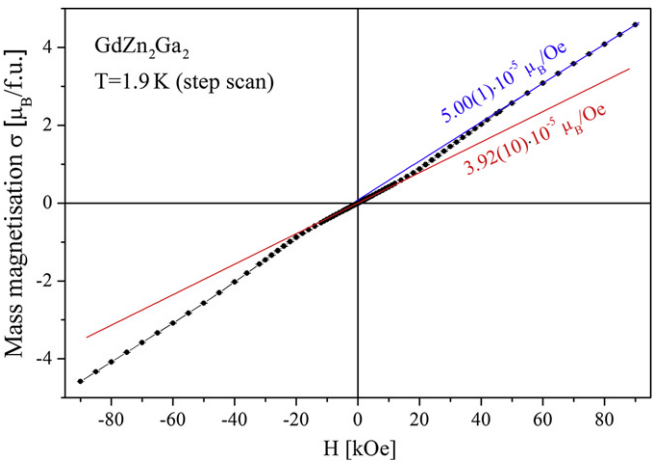

Fig. 4. Field dependence of the mass magnetisation σ isotherm as measured with a PPMS VSM option for $GdZn_2Ga_2$ at $T = 1.9$ K. Straight lines with different slopes ($(3.92(10) \cdot 10^{-5}\ \mu_B$/Oe) and ($5.00(1) \cdot 10^{-5}\ \mu_B$/Oe)) represent the fits to the low and high field magnetisation data. For explanation see text.

Different low ($3.92(10)\cdot10^{-5}\mu_B$/Oe) and high field ($5.00(1)\cdot10^{-5}\mu_B$/Oe) slopes of the fitted straight lines presented in Fig. 4 are indicative for complexity of magnetic structure of the compound under study. The observed behaviour can be ascribe to a first order metamagnetic phase transition of a spin–flop type taking place between 2 and 4 T. Since our measurements were done on polycrystalline bulk sample, such as spin–flop transition is not sharply defined but the complete field alignment of moments is not achieved in the highest applied magnetic field. The value of the magnetic moment at the highest applied field $H_0 = 90$ kOe at $T = 1.9$ K is 59.89 Oe cm^3 g^{-1} or 4.6 μ_B/Gd (or f.u., see Fig. 4) being far from the theoretical saturation moment of gadolinium ($\mu_{sat} = gJ\mu_B = 7\mu_B$).

4. Conclusions

The new ternary intermetallic compound $GdZn_2Ga_2$ was synthesized at ~950 °C and its crystal structure was derived from single crystal X-ray diffraction data. This compound belongs to the well known $BaAl_4$ structure type, *I*4/*mmm* space group, Pearson symbol *tI*10, $Z = 2$. Magnetic measurements show that it is formed with Gd^{3+} ions and orders antiferromagnetically below $T_N = 17.0$ K.

Acknowledgements

This work was partially supported by FCT, Portugal, under the contract No. PTDC/CTM/102766/2008. The FCT Grant No. SFRH/BPD/34840/2007 for the research work of Y.V. at ITN, Sacavém, Portugal is highly appreciated. The magnetic measurements were carried out with the PPMS – Quantum Design equipment purchased thanks to the financial support of the European Regional Development Fund in the framework of the Polish Innovation Economy Operational Program (contract no. POIG.02.01.00–12–023/08).

References

[1] Villars P, editor. Pearson's handbook, crystallographic data for intermetallic phases. OH: ASM Materials Park; 1997.
[2] Parthé E, Gelato L, Chabot B, Penzo M, Cenzual K, Gladyshevskii R. TYPIX, standardized data and crystal chemical characterization of inorganic structure types. Berlin: Springer–Verlag; 1994.
[3] Verbovytskyy Yu, Gonçalves AP. The Yb–Zn–Ga system: partial isothermal section at 400°C with 0–33.3 at.% Yb. Intermetallics 2010;18:655–65.
[4] Verbovytskyy Yu, Pereira LCJ, Gonçalves AP. Crystal structure and magnetic properties of $YbZn_{8.3-9.2}Ga_{2.7-1.8}$ with $BaHg_{11}$. J Alloys Compd 2011;509:L14–7.
[5] Verbovytskyy Yu, Pereira LCJ, Lopes EB, Gonçalves AP. Crystal structure and properties of the new ternary $YbZn_xGa_{4-x}$ and $Yb_3Zn_{11-x}Ga_x$ phases. Intermetallics 2011;19:1989–95.
[6] Verbovytskyy Yu, Kaczorowski D, Gonçalves AP. Novel RZn_2Ga_2 (R = La, Ce, Pr, Nd, Sm) intermetallic compounds with $BaAl_4$ structure type. J Alloys Compd 2010;508:20–3.
[7] Verbovytskyy Yu, Kaczorowski D, Gonçalves AP. On new ternary phases from Eu–Zn–T (T = Al and Ga) systems. Intermetallics 2011;19:613–20.
[8] Verbovytskyy Yu, Leal N, Gonçalves AP. New representatives $BaAl_4$, La_3Al_{11} and $BaHg_{11}$ structure types from the R–Zn–Ga systems (R = Y, Lu, Gd–Tm). Intermetallics 2011;19:1080–4.
[9] Sheldrick GM. SHELX–97, a program system for the solution and refinement of crystal structures. Universität Gött (Germany); 1997.
[10] Bokiy GB. Crystal chemistry. 3rd ed. Moscow: Nauka; 1971 [in Russian].
[11] Czjzek G, Oestreich V, Schmidt H, Łątka K, Tomala K. A study of compounds GdT_2Si_2 by Mössbauer spectroscopy and by bulk magnetization measurements. J Magn Magn Mater 1989;79:42–56.
[12] Freeman AJ. Energy band structure, indirect exchange interaction and magnetic ordering. In: Elliott RJ, editor. Magnetic properties of rare earth metals. London and New York: Plenum Press; 1972. p. 245 [Chapter 6].